GDCh

**Research Articles**

*Angewandte*
*Chemie*
International Edition
www.angewandte.org

*Hybrid Materials*

# Anomalous Charge Transfer from Organic Ligands to Metal Halides in Zero-Dimensional [(C₆H₅)₄P]₂SbCl₅ Enabled by Pressure-Induced Lone Pair-π Interaction

*Hui Luo, Kejun Bu, Yanfeng Yin, Dong Wang, Cuimi Shi, Songhao Guo, Tonghuan Fu, Jiayuan Liang, Bingyan Liu, Dongzhou Zhang, Liang-Jin Xu, Qingyang Hu, Yang Ding, Shengye Jin, Wenge Yang, Biwu Ma, and Xujie Lü\**

**Abstract:** Low-dimensional (low-D) organic metal halide hybrids (OMHHs) have emerged as fascinating candidates for optoelectronics due to their integrated properties from both organic and inorganic components. However, for most of low-D OMHHs, especially the zero-D (0D) compounds, the inferior electronic coupling between organic ligands and inorganic metal halides prevents efficient charge transfer at the hybrid interfaces and thus limits their further tunability of optical and electronic properties. Here, using pressure to regulate the interfacial interactions, efficient charge transfer from organic ligands to metal halides is achieved, which leads to a near-unity photoluminescence quantum yield (PLQY) at around 6.0 GPa in a 0D OMHH, $[(C_6H_5)_4P]_2SbCl_5$. *In situ* experimental characterizations and theoretical simulations reveal that the pressure-induced electronic coupling between the lone-pair electrons of $Sb^{3+}$ and the π electrons of benzene ring (lp-π interaction) serves as an unexpected "bridge" for the charge transfer. Our work opens a versatile strategy for the new materials design by manipulating the lp-π interactions in organic–inorganic hybrid systems.

## Introduction

Organic metal halide hybrids (OMHHs) have attracted widespread interest due to their tunable structures and superior properties that integrate the advantages of both organic and inorganic building blocks.[1] Dimensionality engineering has further enabled the development of materials, ranging from three-dimensional (3D) to two-D (2D), one-D (1D), and even zero-D (0D) at the molecular level.[2] The unique quantum effects and higher stability of the low-D compounds offer tremendous opportunities for the functionality design of OMHHs.[3] Despite significant progress has been made in the exploration of various low-D OMHHs, some fundamental and technological questions remain.[4] A key problem lies in the inferior charge transfer at the organic–inorganic hybrid interfaces, which has been the crucial obstacle to achieve satisfactory performance in the potential applications.

Recently, many efforts have been made in realizing the charge transfer at the hybrid interfaces of 2D and 1D OMHHs by incorporating large conjugated organic molecules into the metal halides.[1e,5] In these cases, the electronic orbitals of the organic molecules extend to band edges and thus form type-II aligned heterostructure where the energy band offset would provide the driving force for charge transfer at the hybrid interfaces. Moreover, the long ammonium chains in these organic molecules can circumvent the limitation of steric hindrance, improving the vertical intercalation with inorganic metal halides. Therefore, the rationally reconfigured band alignments coupled with the reduced distance enable the charge transfer at hybrid interfaces. However, to the best of our knowledge, spontaneous charge transfer at the hybrid interfaces upon photoexcitation in 0D OMHHs, which usually possess higher emission efficiencies and better stability than 2D and 1D compounds, has not been reported yet. This motivates us to

[*] H. Luo, Dr. K. Bu, D. Wang, S. Guo, T. Fu, J. Liang, B. Liu, Prof. Q. Hu, Prof. Y. Ding, Prof. W. Yang, Prof. X. Lü
Center for High Pressure Science and Technology Advanced Research (HPSTAR)
201203 Shanghai (China)
E-mail: xujie.lu@hpstar.ac.cn

Dr. Y. Yin, Prof. S. Jin
State Key Laboratory of Molecular Reaction Dynamics and Dynamics Research Center for Energy and Environmental Materials, Dalian Institute of Chemical Physics, Chinese Academy of Sciences
116023 Dalian, Liaoning (China)

C. Shi, Prof. L.-J. Xu
State Key Laboratory of Structural Chemistry, Fujian Institute of Research on the Structure of Matter, Chinese Academy of Sciences
350002 Fuzhou, Fujian (China)

Dr. D. Zhang
Hawaii Institute of Geophysics and Planetology University of Hawaii Manoa Honolulu
96822 Honolulu, HI (USA)

Prof. B. Ma
Department of Chemistry and Biochemistry, Florida State University
32306 Tallahassee, FL (USA)

manipulate and understand the interfacial behaviors of 0D OMHHs for achieving the efficient charge transfer at their hybrid interfaces.

In this work, we have performed a comprehensive study on the electronic coupling between organic ligands and metal halides in an organic semiconductor-incorporated 0D OMHH $[(C_6H_5)_4P]_2SbCl_5$ (thereafter $(Ph_4P)_2SbCl_5$) under high pressures. At ambient conditions, a type-II energy-level alignment is formed between the organic ligands ($Ph_4P^+$) and inorganic metal halides ($SbCl_5^{2-}$) according to a previous study.[6] Unfortunately, no charge transfer was observed between the organic and inorganic components, despite of the offset of energy levels. Such a case suggests that energy-level offset is insufficient to enable spontaneous charge transfer at the hybrid interfaces of 0D OMHHs, which calls for the creation of new channels and the understanding of the mechanisms. As a thermodynamic variable, pressure provides an effective means to regulate the interfacial interactions by adjusting the atomic and electronic structures.[7] Combining *in situ* experimental diagnostics and theoretical calculations, we have systematically investigated the pressure-dependent evolutions of structure and optical property of $(Ph_4P)_2SbCl_5$ and the underlying mechanisms are elucidated. Surprisingly, compression induces an anomalous interaction between the lone-pair electrons (LPEs) of $Sb^{3+}$ and the $\pi$ electrons of benzene ring (lp-$\pi$ interaction) which brings in a "bridge" for charge transfer. Consequently, the photogenerated electrons and holes could transfer efficiently from organic ligands to inorganic metal halides at the hybrid interface, and eventually gives a near-unity photoluminescence quantum yield (PLQY) via radiative recombination. Our study offers a new strategy to realize efficient charge transfer at the hybrid interfaces of low-D metal halides by modulating lp-$\pi$ interactions, which paves the way toward their potential applications in electronics and optoelectronics.

## Results and Discussion

*In situ* photoluminescence (PL) spectroscopy and fluorescent imaging were performed to explore the variations of emission property in the 0D OMHH $(Ph_4P)_2SbCl_5$ under high pressures. At ambient conditions, $(Ph_4P)_2SbCl_5$ exhibits a broadband emission peaked at 675 nm with a full width at half maximum (FWHM) of 160 nm (Figure S1), which is a typical feature for the radiative recombination of self-trapped excitons (STEs).[4] Both PL spectra (Figure 1a) and fluorescent images (Figures 1b and S2) indicate the significant role of pressure in tuning the emission property.

As PL intensity is not an intrinsic parameter, which can be affected by many factors including excitation laser power and varied absorption, measuring the PLQY values under high pressures is required to quantitatively evaluate the emission property. The analysis methods can be found in the Supporting Information.[8] As shown in Figure 1c, PLQY shows a slight increase during compression, and then rapidly decreases till 2.5 GPa. Intriguingly, a secondary increase of
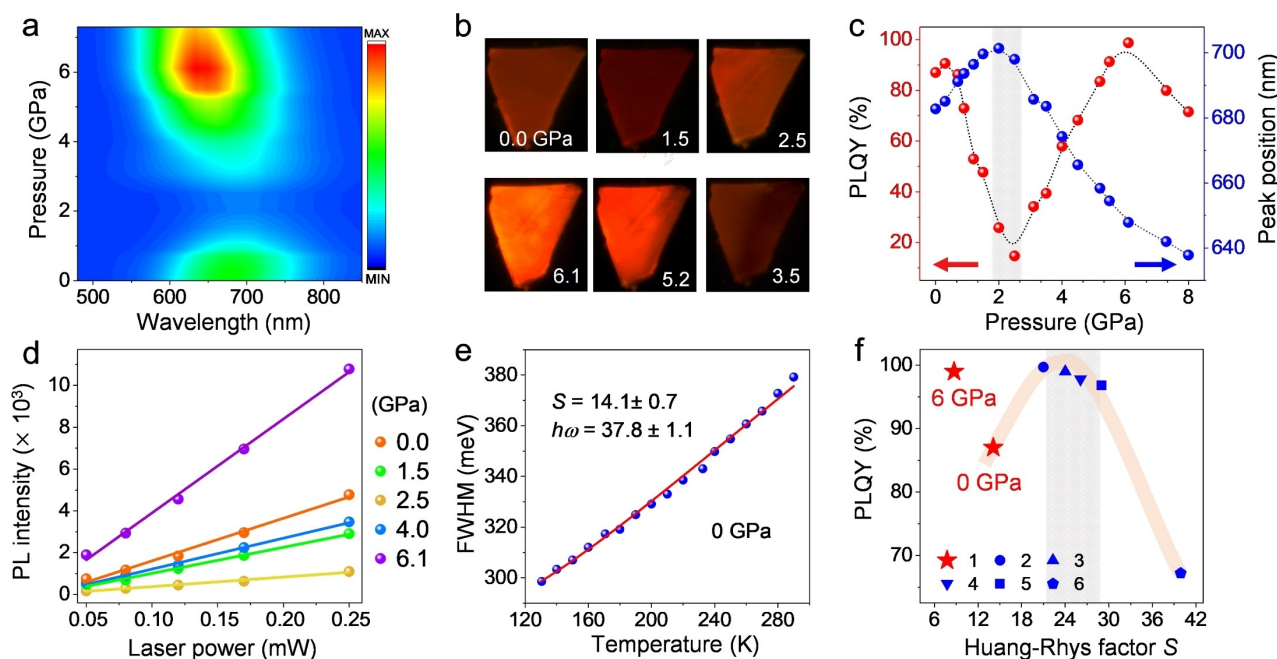


*Figure 1.* (a) The PL spectra of $(Ph_4P)_2SbCl_5$ during compression (excited by 360 nm laser). (b) The fluorescent images at selected pressures under UV irradiation (360–390 nm). (c) The pressure-induced variations of PLQY and PL peak position. (d) Power-law fittings of the power-dependent PL intensity at different pressures. (e) The value of Huang–Rhys factor $S$ of $(Ph_4P)_2SbCl_5$ at ambient conditions, which is determined by the temperature-dependent PL spectroscopy. (f) The relationship between Huang–Rhys factor $S$ and PLQY of $(Ph_4P)_2SbCl_5$ at 6.0 GPa in comparison to that of other Sb–Cl-based OMHHs, which indicate an abnormal behavior of $(Ph_4P)_2SbCl_5$ at 6.0 GPa. 1 to 6 identify the compounds of $(Ph_4P)_2SbCl_5$, $(C_{19}H_{18}P)_2SbCl_5$, $(C_3H_9N)_2SbCl_5 \cdot C_3H_7NO$, $(C_{12}H_{28}N)_2SbCl_5$, $(C_9H_{20}N)_2SbCl_5$, and $(C_{16}H_{28}N)_2SbCl_5$, respectively.[13]

PLQY appears afterwards and reaches the maximum value of 99 % at 6.0 GPa. To rule out the possible contribution from defects, the laser power-dependence PL spectra at different pressures were collected. As shown in Figures 1d and S4, the linear relationship between PL intensity and the excitation laser power suggests that the emission does not come from the defects.[9] On the other hand, we noticed a turnover of the pressure-dependent PL peak position (Figure 1c) at the same pressure for the second enhancement of PLQY. This indicates the possible change of photophysical process in $(Ph_4P)_2SbCl_5$ which we will elaborate on later.

Previous studies have attributed the enhancement of PLQY to the optimized exciton-phonon coupling, which can be quantified by Huang–Rhys factor $S$.[8a,10] In order to achieve a high PLQY, an optimal $S$ value is required.[8b,11] Thus, the $S$ values of $(Ph_4P)_2SbCl_5$ at different pressures were determined by fitting the temperature-dependent FWHM of PL spectra (Figures 1e and S5, Methods in Supporting Information).[8b] For reference, the PLQY-$S$ relations of other Sb–Cl based 0D OMHHs are summarized in Figure 1f,[12] which show that regulating $S$ factor towards 24 would maximize PLQY. Unexpectedly, the $S$ value of $(Ph_4P)_2SbCl_5$ decreases from 14.1 at ambient conditions to 8.7 (Figure S6) at 6.0 GPa, accompanied with the increment of PLQY. The exceptional PLQY-$S$ relationship suggests that the second enhancement of PLQY benefits from other unexplored factor and the corresponding mechanism deserves further investigation.

*In situ* absorption spectra and optical images of $(Ph_4P)_2SbCl_5$ crystal at high pressures were collected to explore the mechanism of second enhancement of PLQY (Figures 2a, b and S7). At ambient conditions, the two absorption edges are ascribed to the absorption of organic ligands (left) and inorganic metal halides (right), respectively. To further support our conclusion, we measured the absorption spectrum of $(Ph_4P)_2ZnCl_4$, which shows an absorption edge determined by the organic $Ph_4P^+$ (Figure S8).[13] During compression, the absorption of metal halides exhibits a blue shift up to 2.5 GPa, and then turns to red shift. On the other hand, the absorption of organic ligands shows a continuous redshift. It is worth noting that the two absorption edges merge at 6.0 GPa, suggesting the similar energy gap of ligands and metal halides. At this situation, the photoexcited carriers would distribute in both organic ligands and metal halides, and thus the emissions from both $SbCl_5^{2-}$ metal halides and $Ph_4P^+$ ligands are supposed to be detected. However, only the emission from $SbCl_5^{2-}$ metal halides is detected (Figures S9 and S10), which rules out the possibility that the excited carriers recombine in ligands.[13] Taking the consideration of near-unity PLQY at 6.0 GPa, the photogenerated carriers in the ligands are believed to transfer across the hybrid interface to the metal halides.

To verify our statement, the pressure-regulated femtosecond transient absorption (fs-TA) spectroscopy was conducted, which is a powerful technique that has been broadly used to probe photo-excited state dynamics. At ambient
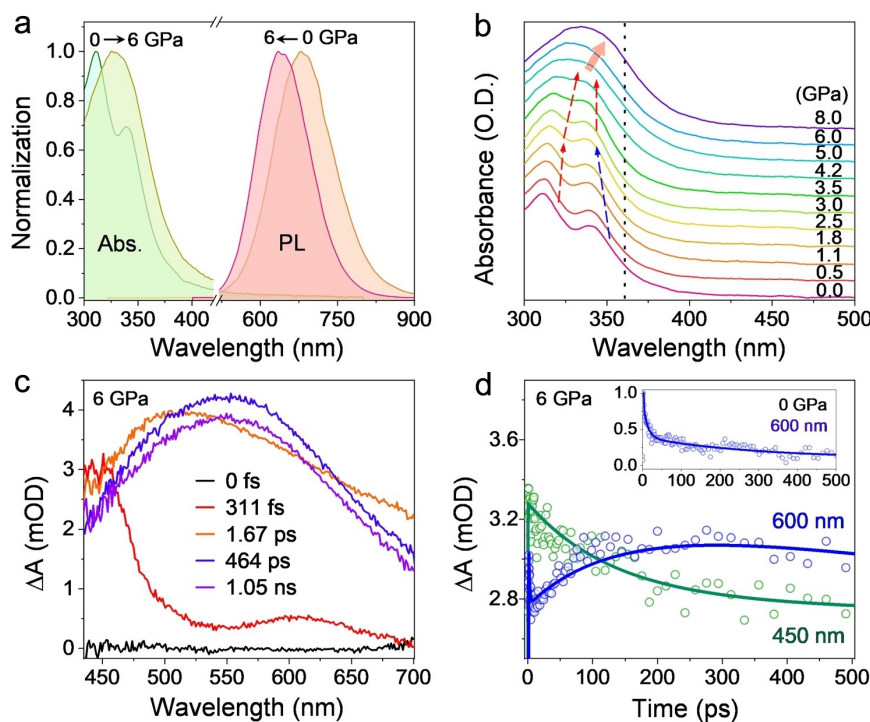


**Figure 2.** (a) The absorption and emission spectra of $(Ph_4P)_2SbCl_5$ at ambient pressure and 6.0 GPa. (b) The pressure-induced variations of absorption spectra. (c) The femtosecond transient absorption (TA) spectra of $(Ph_4P)_2SbCl_5$ at different delay times under excitation at 360 nm. (d) The TA kinetics of $(Ph_4P)_2SbCl_5$ at 6.0 GPa probed at 450 and 600 nm. Solid lines are fits to the kinetics by a multiexponential function. The inset shows the decay dynamics probed at 600 nm at ambient pressure.

*Angew. Chem. Int. Ed.* **2023**, 62, e202304494 (3 of 6)

© 2023 Wiley-VCH GmbH

conditions, a broad photo-induced absorption (PIA) signal emerges immediately excited by a 360 nm laser (Figure S11a), which provides direct evidence on the existence of STEs.[14] Figure 2c shows the TA spectra at different delay times at 6.0 GPa where a new PIA signal ($\approx 450$ nm) rises rapidly (311 fs) on the time scale of the instrument response (200 fs), which is absent as depicted in Figure S11b at ambient conditions. The wavelength-dependent time-resolved PL spectra in Figure S12 rule out the possibility of the new PIA signal originated from pressure-induced different self-trapped states of metal halides.[15] Therefore, the new PIA signal is ascribed to the formation of excited carriers in the ligands.[5b] The dynamics of the ligand PIA (probed at 450 nm) and metal halide PIA (probed at 600 nm) are shown in Figure 2d. By means of the global fitting, the rise time (140 ps) of the metal halide PIA coincides with the decay time scale of the ligand PIA (132 ps), suggesting the transfer of the excited carriers from ligands to metal halides.[16] In the meanwhile, the rise of metal halide PIA is absent at ambient conditions (inset of Figure 2d), which confirms the charge transfer at the interface.

The ligand-to-metal halide charge transfer is believed to be closely linked to the variations of crystal and electronic structures of $(Ph_4P)_2SbCl_5$. We first traced the evolution of the crystal structure under high pressure using *in situ* synchrotron X-ray diffraction (XRD). The ambient pressure crystal structure of $(Ph_4P)_2SbCl_5$ is shown in Figure 3a where the individual $SbCl_5^{2-}$ pyramids are surrounded by the large tetrahedral $Ph_4P^+$ cations. Figure 3b presents the selected XRD patterns under high pressures where all Bragg diffraction peaks continuously shift to the large 2θ direction due to the lattice contraction and no new peaks are observed. The variations of lattice constants and unit-cell volume under pressure were refined by the Rietveld methods and the detailed analysis and discussion can be found in the Supporting Information (Figures S13 and S14, Table S1). By fitting the unit-cell volume to the Birch-Murnaghan equation of state,[17] an inflection point can be observed which may be attributed to the generation of lone pair-π (lp-π) interaction at high pressures.

Lp-π interaction is a counterintuitive intermolecular force which takes place between lone pair-bearing electronegative atoms of the neutral molecules and π-acidic aromatic systems.[18] Previous studies have revealed that the strength of lp-π interaction relies on the spacing and relative orientation of the lone-pair atom and π-system.[19] To better describe the pressure-induced lp-π interaction at the interfaces, we calculate the average distance between six C and Sb atoms as well as the corresponding variance (Table S2). At ambient conditions, the interfacial distance is as long as 5.7 Å which inhibits the interaction between ligands and metal halides. During compression, the distance decreases to 4.6 Å at 6.0 GPa (Figure 3c). The direct visualization of the variations during compression can be seen from the inset in Figure 3c. To further elucidate the nature of the interaction between lone-pair atoms and π-systems, the electron localization function (ELF) of $(Ph_4P)_2SbCl_5$ was calculated under
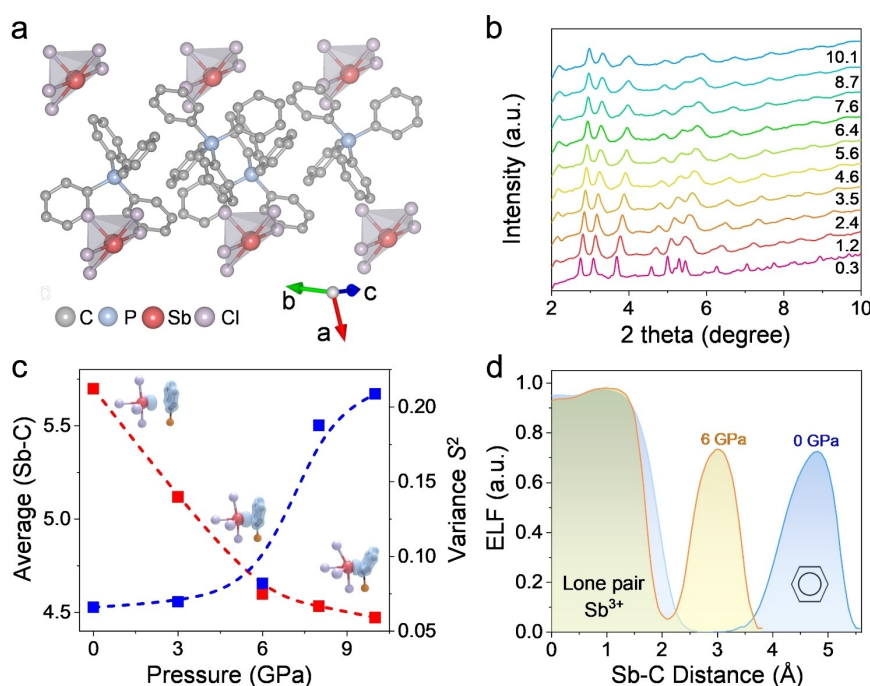


***Figure 3.*** (a) Crystal structure of $(Ph_4P)_2SbCl_5$ at ambient conditions (red spheres, antimony atoms; purple spheres, chloride atoms; blue spheres, phosphorus atoms; gray spheres, carbon atoms; mauve polyhedral, $SbCl_5^{2-}$; hydrogen atoms are hidden for clarity). (b) XRD patterns of $(Ph_4P)_2SbCl_5$ at selected pressures. (c) The variations of average distance (red line) between six C and Sb, as well as the corresponding variance (blue line). Inset illustrates the interaction between lone-pair electrons of $Sb^{3+}$ and π electrons of benzene ring. (d) The ELF line profiles between Sb and benzene rings at ambient pressure and at 6.0 GPa.

high presures. The ELF line profiles connecting specific atoms are plotted in Figure 3d to highlight the the relation between $Sb^{3+}$ and benzene ring. There is no interaction between $Sb^{3+}$ and benzene ring at ambient conditions owing to the long interfacial distance. When pressure reaches to 6.0 GPa, the interfacial distance reduces and the overlap of electron clouds between $Sb^{3+}$ and benzene ring appears, indicating the formation of lp-π interaction. Consequently, the pressure-induced lp-π interaction serves as a "bridge" for the high efficiency of charge transfer from organic ligands to metal halides, giving rise to high emission.

The behavior of the excited carriers at the interfaces is heavily dependent on the energy-level alignments. Type-I energy-level alignment is characterized by the lowest unoccupied molecular orbital (LUMO) and highest occupied molecular orbital (HOMO) being determined solely by the organic ligands or metal halides. While type-II energy-level alignment involves the HOMO and LUMO from different components. To understand the electronic origin of inter-facial charge transfer in $(Ph_4P)_2SbCl_5$, the HOMO and LUMO of ligands and metal halides were calculated by first-principles calculations (Figure S15). At ambient conditions, $(Ph_4P)_2SbCl_5$ exhibits a type-II energy-level alignment with a relatively large energy-level offsets $\Delta E_{HOMO}$ and $\Delta E_{LUMO}$ (Figure 4a), in line with the reported theoretical result.[6] In this case, the photogenerated carriers should be separated at the interface. However, the weak interfacial interaction stands as a hurdle for the charge transfer (Figure 4c). Upon compression, the reduction Sb–Cl bond length in $(Ph_4P)_2SbCl_5$ increases the overlap of electron orbitals (Table S3). This leads to a decrease in the LUMO energy level of metal halides, reaching the energy level of the

organic ligands beyond 6.0 GPa (Figures 4b and S16). Consequently, the pressure-induced formation of a quasi-type-I energy-level alignment provides driving force for the photoexcited carriers transferring from ligands to metal halides. Therefore, the excited carriers would transfer from organic $Ph_4P^+$ ligands to $SbCl_5^{2-}$ metal halides with the help of pressure-induced lp-π interaction which serves as a new channel for the charge transfer at the hybrid interface (Figure 4d). This results in a high radiative recombination at metal halides.

## Conclusion

In summary, anomalously efficient charge transfer from organic ligands to metal halides has been achieved in a 0D organic metal halide hybrid $(Ph_4P)_2SbCl_5$ with pressure tuning. Through a comprehensive *in situ* experimental characterization combined with theoretical calculations, we have elucidated the underlying mechanisms for the efficient ligand-to-metal halide charge transfer and its significant contributions to the modulation of emission properties. The pressure-induced coupling between the lone-pair electrons of $Sb^{3+}$ and the π electrons of benzene ring (lp-π interaction) serves as the "bridge" for the charge transfer at the organic–inorganic interfaces. In addition, the pressure-induced transition of energy-level alignment from type-II to quasi-type-I provides driving force for the charge transfer from ligands to metal halides, together resulting in the high emission with a 99 % PLQY at the metal halides. Our study not only achieves efficient interfacial charge transfer and near-unity PLQY in a 0D OMHH but also opens a versatile
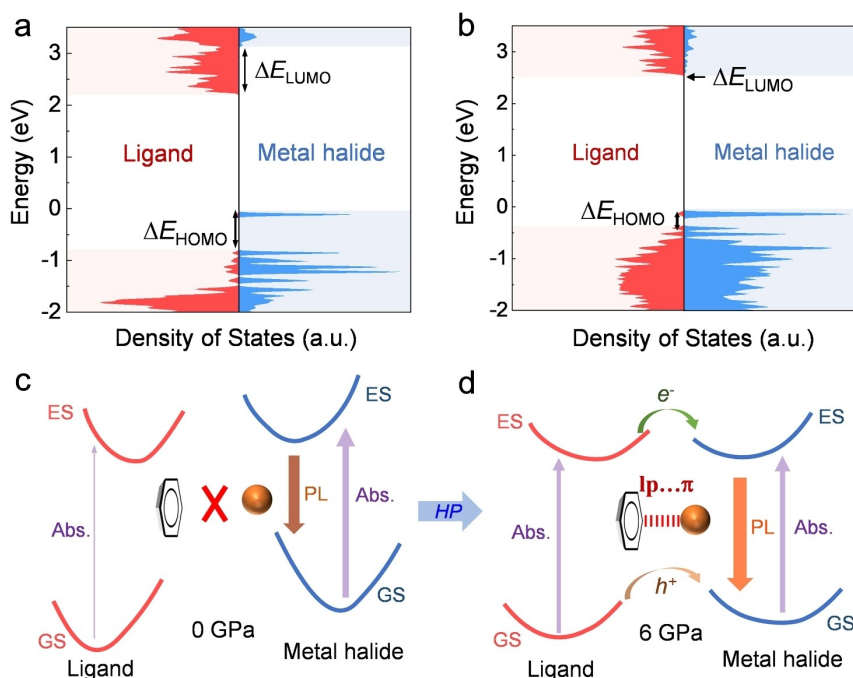


***Figure 4.*** (a, b) Calculated partial density of state for the organic ligands (red) and inorganic metal halides (blue) at different pressures. (c, d) Schematic diagram of the pressure-induced transformation of carrier dynamics in $(Ph_4P)_2SbCl_5$ (GS, ground state; ES, excited state).

strategy for the design of hybrid materials by engineering the lp-π interaction which has previously been under-investigated.

## Conflict of Interest

The authors declare no conflict of interest.

## Data Availability Statement

The data that support the findings of this study are available in the supplementary material of this article.

[1] a) A. Kojima, K. Teshima, Y. Shirai, T. Miyasaka, *J. Am. Chem. Soc.* **2009**, *131*, 6050–6051; b) M. Grätzel, *Nature* **2003**, *421*, 586–587; c) S. Reineke, F. Lindner, G. Schwartz, N. Seidler, K. Walzer, B. Lüssem, K. Leo, *Nature* **2009**, *459*, 234–238; d) M. Faustini, L. Nicole, E. Ruiz-Hitzky, C. Sanchez, *Adv. Funct. Mater.* **2018**, *28*, 1704158; e) Y. Gao, E. Shi, S. Deng, S. B. Shiring, J. M. Snaider, C. Liang, B. Yuan, R. Song, S. M. Janke, A. Liebman-Peláez, P. Yoo, M. Zeller, B. W. Boudouris, P. Liao, C. Zhu, V. Blum, Y. Yu, B. M. Savoie, L. Huang, L. Dou, *Nat. Chem.* **2019**, *11*, 1151–1157.

[2] a) M. J. Katz, K. Sakai, D. B. Leznoff, *Chem. Soc. Rev.* **2008**, *37*, 1884–1895; b) P. Gao, A. R. Bin Mohd Yusoff, M. K. Nazeeruddin, *Nat. Commun.* **2018**, *9*, 5028; c) R. Quintero-Bermudez, A. Gold-Parker, A. H. Proppe, R. Munir, Z. Yang, S. O. Kelley, A. Amassian, M. F. Toney, E. H. Sargent, *Nat. Mater.* **2018**, *17*, 900–907; d) X. Lü, C. Stoumpos, Q. Hu, X. Ma, D. Zhang, S. Guo, J. Hoffman, K. Bu, X. Guo, Y. Wang, C. Ji, H. Chen, H. Xu, Q. Jia, W. Yang, M. G. Kanatzidis, H.-K. Mao, *Natl. Sci. Rev.* **2021**, *8*, nwaa288.

[3] a) C. Katan, N. Mercier, J. Even, *Chem. Rev.* **2019**, *119*, 3140–3192; b) M. S. Cao, X. X. Wang, M. Zhang, J. C. Shu, W. Q. Cao, H. J. Yang, X. Y. Fang, J. Yuan, *Adv. Funct. Mater.* **2019**, *29*, 1807398.

[4] M. Li, Z. Xia, *Chem. Soc. Rev.* **2021**, *50*, 2626–2662.

[5] a) J. Xue, R. Wang, X. Chen, C. Yao, X. Jin, K. L. Wang, W. Huang, T. Huang, Y. Zhao, Y. Zhai, D. Meng, S. Tan, R. Liu, Z. K. Wang, C. Zhu, K. Zhu, M. C. Beard, Y. Yan, Y. Yang, *Science* **2021**, *371*, 636–640; b) E. Amerling, Y. Zhai, B. W. Larson, Y. Yao, B. Fluegel, Z. Owczarczyk, H. Lu, L. Whittaker-Brooks, V. Blum, J. L. Blackburn, *J. Mater. Chem. A* **2021**, *9*, 14977–14990; c) S. Guo, Y. Li, Y. Mao, W. Tao, K. Bu, T. Fu, C. Zhao, H. Luo, Q. Hu, H. Zhu, E. Shi, W. Yang, L. Dou, X. Lü, *Sci. Adv.* **2022**, *8*, eadd1984.

[6] C. Zhou, M. Worku, J. Neu, H. Lin, Y. Tian, S. Lee, Y. Zhou, D. Han, S. Chen, A. Hao, P. I. Djurovich, T. Siegrist, M. H. Du, B. Ma, *Chem. Mater.* **2018**, *30*, 2374–2378.

[7] a) Z. Wang, C. Schliehe, T. Wang, Y. Nagaoka, Y. C. Cao, W. A. Bassett, H. Wu, H. Fan, H. Weller, *J. Am. Chem. Soc.* **2011**, *133*, 14484–14487; b) F. Bai, K. Bian, X. Huang, Z. Wang, H. Fan, *Chem. Rev.* **2019**, *119*, 7673–7717.

[8] a) Y. Wang, S. Guo, H. Luo, C. Zhou, H. Lin, X. Ma, Q. Hu, M. H. Du, B. Ma, W. Yang, X. Lü, *J. Am. Chem. Soc.* **2020**, *142*, 16001–16006; b) H. Luo, S. Guo, Y. Zhang, K. Bu, H. Lin, Y. Wang, Y. Yin, D. Zhang, S. Jin, W. Zhang, W. Yang, B. Ma, X. Lü, *Adv. Sci.* **2021**, *8*, 2100786.

[9] E. R. Dohner, A. Jaffe, L. R. Bradshaw, H. I. Karunadasa, *J. Am. Chem. Soc.* **2014**, *136*, 13154–13157.

[10] a) Q. Li, Z. Chen, B. Yang, L. Tan, B. Xu, J. Han, Y. Zhao, J. Tang, Z. Quan, *J. Am. Chem. Soc.* **2020**, *142*, 1786–1791; b) Y. Shi, Z. Ma, D. Zhao, Y. Chen, Y. Cao, K. Wang, G. Xiao, B. Zou, *J. Am. Chem. Soc.* **2019**, *141*, 6504–6508.

[11] S. Li, J. Luo, J. Liu, J. Tang, *J. Phys. Chem. Lett.* **2019**, *10*, 1999–2007.

[12] a) J.-L. Li, Y.-F. Sang, L.-J. Xu, H.-Y. Lu, J.-Y. Wang, Z.-N. Chen, *Angew. Chem. Int. Ed.* **2022**, *61*, e202113450; b) L. Lian, P. Zhang, X. Zhang, Q. Ye, W. Qi, L. Zhao, J. Gao, D. Zhang, J. Zhang, *ACS Appl. Mater. Interfaces* **2021**, *13*, 58908–58915; c) C. Zhou, H. Lin, Y. Tian, Z. Yuan, R. Clark, B. Chen, L. J. van de Burgt, J. C. Wang, Y. Zhou, K. Hanson, Q. J. Meisner, J. Neu, T. Besara, T. Siegrist, E. Lambers, P. Djurovich, B. Ma, *Chem. Sci.* **2018**, *9*, 586–593; d) H. Peng, Y. Tian, Z. Yu, X. Wang, B. Ke, Y. Zhao, T. Dong, J. Wang, B. J. S. C. M. Zou, *Sci. China Mater.* **2022**, *65*, 1594–1600; e) T. Chang, Q. Wei, R. Zeng, S. Cao, J. Zhao, B. Zou, *J. Phys. Chem. Lett.* **2021**, *12*, 1829–1837.

[13] L. J. Xu, A. Plaviak, X. Lin, M. Worku, Q. He, M. Chaaban, B. J. Kim, B. Ma, *Angew. Chem. Int. Ed.* **2020**, *59*, 23067–23071.

[14] B. Yang, K. Han, *J. Phys. Chem. Lett.* **2021**, *12*, 8256–8262.

[15] J. E. Thomaz, K. P. Lindquist, H. I. Karunadasa, Fayer, M. D. Fayer, *J. Am. Chem. Soc.* **2020**, *142*, 16622–16631.

[16] X. Tang, L. S. Cui, H. C. Li, A. J. Gillett, F. Auras, Y. K. Qu, C. Zhong, S. T. E. Jones, Z. Q. Jiang, R. H. Friend, L. S. Liao, *Nat. Mater.* **2020**, *19*, 1332–1338.

[17] F. Birch, *Phys. Rev.* **1947**, *71*, 809–824.

[18] J.-J. Liu, Y.-F. Guan, Y. Chen, M.-J. Lin, C.-C. Huang, W.-X. Dai, *Dalton Trans.* **2015**, *44*, 17312–17317.

[19] a) J. Z. Liao, J. F. Chang, L. Meng, H. L. Zhang, S. S. Wang, C. Z. Lu, *Chem. Commun.* **2017**, *53*, 9701–9704; b) T. J. Mooibroek, P. Gamez, J. Reedijk, *CrystEngComm* **2008**, *10*, 1501–1515.